Underwater Image Enhancement with Hyper-Laplacian Reflectance Priors (Supplementary Material)

Peixian Zhuang, Jiamin Wu, Fatih Porikli *Fellow, IEEE*, and Chongyi Li*

***Abstract*— In this supplementary material, we provides 1) iterative half thresholding algorithm, 2) convergence proof of proposed algorithm, 3) more experimental results including color correction validation, convergence analysis, parameter evaluation, and application tests.**

We provide an enhancement experiment on a challenging underwater video including 1500 frames with different types of degenerate colors in a separate file. This video can be found at YouTube https://www.youtube.com/watch?v=KRxKbhYfSLY or Github https://github.com/zhuangpeixian/HLRP.

I. Iterative Half Thresholding Algorithm

Thanks to the literatures [1], [2], we present the definition of iterative half thresholding algorithm for Eq. (14) in our manuscript. The nonconvex optimization model concerned with the $l_{1/2}$ regularization is summarized:

$$\theta_v(\mathbf{x}) = \min_{\mathbf{x}} \|\mathbf{x}-\mathbf{y}\|_2^2 + v\|\mathbf{x}\|_{1/2}, \tag{1}$$

where $v > 0$ is a regularization parameter. In [1], [2], an iterative half thresholding algorithm is developed to find the solution to Eq. (1), and the algorithm is detailed below.

<u>**Lemma 1**</u>. With any real parameter $\mu \in (0, 1/N)$, any minimizer $\mathbf{x}^*$ of Eq. (1) satisfies

$$\mathbf{x}^* = \mathbf{H}_{v\mu,\frac{1}{2}}(\mathbf{x}^* - \mu(\mathbf{x}^* - \mathbf{y})), \tag{2}$$

where N is the total pixel number of $\mathbf{x}$, and $\mathbf{H}_{v\mu,\frac{1}{2}}(\cdot)$ is the half thresholding operator defined by

$$\mathbf{H}_{v\mu,\frac{1}{2}}(\mathbf{z}) = (\mathbf{f}_{v\mu,\frac{1}{2}}(z_1), ..., \mathbf{f}_{v\mu,\frac{1}{2}}(z_N))^T, \quad \forall \mathbf{z} \in R^N, \tag{3}$$

with

$$\mathbf{f}_{v\mu,\frac{1}{2}}(z_i) = \begin{cases} \frac{2}{3} z_i (1 + \cos(\frac{2\pi}{3} - \frac{2}{3}\phi_{v\mu}(z_i))), & |z_i| > \frac{\sqrt[3]{54}}{4}(v\mu)^{\frac{2}{3}} \\ 0, & \text{otherwise} \end{cases}, \tag{4}$$

and $\phi_{v\mu}(z_i) = \arccos(\frac{v\mu}{8}(\frac{|z_i|}{3})^{-\frac{3}{2}})$ for $i = 1, 2, ..., N$.

Based on the thresholding representation Eq. (2), an iterative half thresholding algorithm for the solution to Eq. (1) is naturally defined:

$$\mathbf{x}^{k+1} = \mathbf{H}_{v\mu,\frac{1}{2}}(\mathbf{x}^k - \mu(\mathbf{x}^k - \mathbf{y})), \tag{5}$$

*Corresponding authors (chongyi.li@ntu.edu.sg).

The convergence of the algorithm is partially analyzed in [2] where this algorithm can converge to a stationary point of Eq. (2) when μ is small enough.

II. Convergence Proof of Proposed Algorithm

Thanks to the literatures [1], [2], [3], we provide a convergence proof of the proposed algorithm. The complex problem Eq. (9) in our manuscript is equivalently transformed into two simple subproblems:

Given $\mathbf{R}$, update $\mathbf{I}$ by

$$\min_{\mathbf{I}} \|\mathbf{R} \odot \mathbf{I} - \mathbf{V}\|_2^2 + \zeta_1\|\triangledown \mathbf{I}\|_2^2 + \zeta_2\|\triangle \mathbf{I}\|_2^2 \ \text{ s.t. } \mathbf{V} \leqslant \mathbf{I}, \tag{6}$$

Given $\mathbf{I}$, update $\mathbf{R}$ by

$$\min_{\mathbf{R}} \|\mathbf{R} \odot \mathbf{I} - \mathbf{V}\|_2^2 + \lambda_1\|\triangledown \mathbf{R}\|_{1/2} + \lambda_2\|\triangle \mathbf{R}\|_{1/2}, \tag{7}$$

We find that (6) is a least square problem with three convex functions, consequently, a close-form solution Eq. (15) in our manuscript is derived by taking operations of first-order derivative, least square, and fast Fourier transform. A constraint is addressed by correcting the estimated illumination with numerical comparison described above. We attempt to prove the convergence of (7) as the key problem. As described above, (7) is rewritten by introducing two auxiliary variables $\mathbf{d}$ and $\mathbf{h}$,

$$\begin{aligned} \min_{(\mathbf{R},\mathbf{d},\mathbf{h})} & \|\mathbf{R} \odot \mathbf{I} - \mathbf{V}\|_2^2 + \lambda_1\|\mathbf{d}\|_{1/2} + \lambda_2\|\mathbf{h}\|_{1/2} \\ & \text{s.t. } \ \mathbf{d} = \triangledown \mathbf{R}, \ \mathbf{h} = \triangle \mathbf{R}, \end{aligned} \tag{8}$$

The equivalent augmented Lagrangian functional is deduced with previously defined Lagrange multipliers $\mathbf{m}$ and $\mathbf{n}$ to solve the constrained problem (8),

$$\begin{aligned} \min_{(\mathbf{R},\mathbf{d},\mathbf{h},\mathbf{m},\mathbf{n})} & \left\|\mathbf{R} - \frac{\mathbf{V}}{\mathbf{I}}\right\|_2^2 + \lambda_1\{\eta_1\|\mathbf{d}\|_{1/2} + \|\triangledown \mathbf{R} - \mathbf{d} + \mathbf{m}\|_2^2\} \\ & + \lambda_2\{\eta_2\|\mathbf{h}\|_{1/2} + \|\triangle \mathbf{R} - \mathbf{h} + \mathbf{n}\|_2^2\}, \end{aligned} \tag{9}$$

As previously described, (9) is transformed into the two simple subproblems Eq. (11) and Eq. (12) in our manuscript that can be individually and iteratively optimized. It is worth noting that Eq. (12) in our manuscript is a least square problem with three l_2 norm functions, and a close-form solution Eq. (15) in our manuscript is yielded by implementing operations of first-order derivative, least square, and fast Fourier transform. The nonconvex subproblem Eq. (11) with the $l_{1/2}$ norm in our manuscript is naturally summarized to be the unified form of Eq. (1). We just need to prove the convergence of the iterative half algorithm Eq. (2) as the key problem in the following.

On the basis of the literatures [1], [2], the convergence of the iterative half algorithm to a stationary point of Eq. (2) is first justified, and then the convergence of the algorithm to a local minimizer of Eq. (1) is proved.

Lemma 2. Suppose that $\{\mathbf{x}^k\}$ is the sequence yielded by the iterative half thresholding algorithm and the step size μ satisfies $0 < \mu < 1/N$, then $\mathbf{x}^k$ converges to a stationary point of Eq. (2).

Proof: We prove **Lemma 2** like that of **Theorem 3** in [2]. Some known claims in [2] are first reviewed.

Claim 1: Let $\{\mathbf{x}^k\}$ be the sequence yielded by the iterative half thresholding algorithm with the step size μ meeting $0 < \mu < 1/N$, and $\theta_v(\mathbf{x}) = \|\mathbf{x}-\mathbf{y}\|_2^2 + v\|\mathbf{x}\|_{1/2}$. Then (1) $\{\mathbf{x}^k\}$ is a minimization sequence and $\theta_v(\mathbf{x}^k)$ converges to $\theta_v(\mathbf{x}^*)$ with any limit point of $\{\mathbf{x}^k\}$; (2) $\{\mathbf{x}^k\}$ is asymptotically regular, such that $\lim_{k\to\infty}\|\mathbf{x}^{k+1}-\mathbf{x}^k\|_2 = 0$.

Based on **Claim 1**, it is easily concluded that the iterative half thresholding algorithm is convergent subsequentially.

Claim 2: Under the setting of **Claim 1**, any limit point of $\{\mathbf{x}^k\}$ is a stationary point of Eq. (2).

Let $T_{v,\mu}(\mathbf{x},\mathbf{z}) = \|\mathbf{z}-(\mathbf{x}-\mu(\mathbf{x}-\mathbf{y}))\|_2^2 + v\|\mathbf{z}\|_{1/2}$ and $D_{v,\mu}(\mathbf{x}) = T_{v,\mu}(\mathbf{x},\mathbf{x}) - \min_{\mathbf{z}\in R^N} T_{v,\mu}(\mathbf{x},\mathbf{z})$. By $D_{v,\mu}(\mathbf{x}) \geq 0$ and **Lemma 1**, we have $D_{v,\mu}(\mathbf{x}) \geq 0$ only if $\mathbf{x} = \mathbf{H}_{v\mu,\frac{1}{2}}(\mathbf{x} - \mu(\mathbf{x}-\mathbf{y}))$.

Suppose that $\mathbf{x}^*$ is a limit point of $\{\mathbf{x}^k\}$, there exists a subsequence $\{\mathbf{x}^{k_j}\}$, such that $\mathbf{x}^{k_j} \to \mathbf{x}^*$ when $j\to\infty$. Since $\mathbf{x}^{k_j+1} = \mathbf{H}_{v\mu,\frac{1}{2}}(\mathbf{x}^{k_j} - \mu(\mathbf{x}^{k_j}-\mathbf{y}))$, we derive

$$\begin{aligned} D_{v,\mu}(\mathbf{x}^{k_j}) &= 2\langle \mu(\mathbf{x}^{k_j}-\mathbf{y}), \mathbf{x}^{k_j}-\mathbf{x}^{k_j+1}\rangle \\ &\quad + v\mu(\|\mathbf{x}^{k_j}\|_{1/2} - \|\mathbf{x}^{k_j+1}\|_{1/2}) - \|\mathbf{x}^{k_j}-\mathbf{x}^{k_j+1}\|_2^2, \end{aligned} \tag{10}$$

with implies that

$$\begin{aligned} & v\|\mathbf{x}^{k_j}\|_{1/2} - v\|\mathbf{x}^{k_j+1}\|_{1/2} \\ &= \frac{1}{\mu}\|\mathbf{x}^{k_j}-\mathbf{x}^{k_j+1}\|_2^2 + \frac{1}{\mu}D_{v,\mu}(\mathbf{x}^{k_j}) + 2\langle(\mathbf{x}^{k_j}-\mathbf{y}), \mathbf{x}^{k_j+1}-\mathbf{x}^{k_j}\rangle, \end{aligned} \tag{11}$$

then it follows that

$$\begin{aligned} & \theta_v(\mathbf{x}^{k_j}) - \theta_v(\mathbf{x}^{k_j+1}) \\ &= \frac{1}{\mu}D_{v,\mu}(\mathbf{x}^{k_j}) + \frac{1}{\mu}\|\mathbf{x}^{k_j}-\mathbf{x}^{k_j+1}\|_2^2 - \|\mathbf{x}^{k_j}-\mathbf{x}^{k_j+1}\|_2^2 \\ &\geq \frac{1}{\mu}D_{v,\mu}(\mathbf{x}^{k_j}) + (\frac{1}{\mu}-N)\|\mathbf{x}^{k_j}-\mathbf{x}^{k_j+1}\|_2^2, \end{aligned} \tag{12}$$

due to $0<\mu<1/N$, we compute

$$D_{v,\mu}(\mathbf{x}^{k_j}) \leq \mu(\theta_v(\mathbf{x}^{k_j}) - \theta_v(\mathbf{x}^{k_j+1})), \tag{13}$$

and by **Claim 1**, when $j\to\infty$, we derive

$$\theta_v(\mathbf{x}^{k_j}) - \theta_v(\mathbf{x}^{k_j+1}) \to 0, \tag{14}$$

this indicates that $D_{v,\mu}(\mathbf{x}^*) = 0$, and $\mathbf{x}^* = \mathbf{H}_{v\mu,\frac{1}{2}}(\mathbf{x}^* - \mu(\mathbf{x}^*-\mathbf{y}))$.

Claim 3: The number of stationary points of Eq. (2) is finite.

With **Claims 1 and 2**, it is concluded that the iterative half thresholding algorithm subsequentially converges to a stationary point of Eq. (2). With **Claim 3**, any stationary point of Eq. (2) is isolated with the asymptotic regularity of the sequence in **Claim 1**(2), suggesting that the sequence of $\{\mathbf{x}^k\}$ must be globally convergent to a stationary point. Therefore, the proof of **Lemma 2** is completed.

Theorem 1. Suppose that the step size $0 < \mu < 1/N$ and the sequence $\{\mathbf{x}^k\}$ yielded by the iterative half thresholding algorithm converges to $\mathbf{x}^*$. Let $\Omega = supp(\mathbf{x}^*)$ and $e = \min_{i\in\Omega}|\mathbf{x}_i^*|$. If $\sigma_{\min}(\mathbf{1}_\Omega^T\mathbf{1}_\Omega) > 0$ and $0 < v < 8e^{\frac{3}{2}}\sigma_{\min}(\mathbf{1}_\Omega^T\mathbf{1}_\Omega)$, then there exists $\beta_0\in(0,1)$ for any $\mathbf{x}$ that satisfies $\|\mathbf{x}-\mathbf{x}^*\|_2 < \beta_0 e$, there holds $\theta_v(\mathbf{x}) - \theta_v(\mathbf{x}^*) \geq 0$, that is, $\mathbf{x}^*$ is a local minimizer of Eq. (1).

Proof: Denote $\beta^* = 1 - (\frac{v}{8e^{\frac{3}{2}}\sigma_{\min}(\mathbf{1}_\Omega^T\mathbf{1}_\Omega)})^{\frac{2}{3}}$, and due to $0 < v < 8e^{\frac{3}{2}}\sigma_{\min}(\mathbf{1}_\Omega^T\mathbf{1}_\Omega)$, we deduce $0<\beta^*<1$. For any $\beta\in(0,1)$, we define

$$c_\beta = \frac{1}{(\frac{\sqrt[3]{54}}{2(v\mu)^{\frac{1}{3}}} + \frac{2}{v}\|\mathbf{1}_{\Omega^c}^T\mathbf{1}_\Omega\|_2\beta e)^2 e}, \tag{15}$$

With respect to β, c_β is decreasing monotonically, there is a β_0 that satisfies $\beta_0\leq\beta^*$ and $\beta_0\leq c_{\beta_0}$. When $\|\mathbf{r}\|_2 < \beta_0 e$, it holds $\theta_v(\mathbf{x}^*+\mathbf{r}) - \theta_v(\mathbf{x}^*) \geq 0$.

Actually, we compute

$$\begin{aligned} & \theta_v(\mathbf{x}^*+\mathbf{r}) - \theta_v(\mathbf{x}^*) \\ &= 2\mathbf{r}^T(\mathbf{x}^*-\mathbf{y}) + \mathbf{r}^T\mathbf{r} + v\sum_{i=1}^N(|\mathbf{x}_i^*+\mathbf{r}_i|^{\frac{1}{2}} - |\mathbf{x}_i^*|^{\frac{1}{2}}) \\ &= v\sum_{i=1}^N(|\mathbf{x}_i^*+\mathbf{r}_i|^{\frac{1}{2}} - |\mathbf{x}_i^*|^{\frac{1}{2}} + \frac{2}{v}\mathbf{1}_i^T(\mathbf{x}^*-\mathbf{y})\mathbf{r}_i) + \mathbf{r}^T\mathbf{r} \\ &= v\sum_{i\in\Omega}(|\mathbf{x}_i^*+\mathbf{r}_i|^{\frac{1}{2}} - |\mathbf{x}_i^*|^{\frac{1}{2}} + \frac{2}{v}\mathbf{1}_i^T(\mathbf{x}^*-\mathbf{y})\mathbf{r}_i) \\ &\quad + v\sum_{i\in\Omega^c}(|\mathbf{r}_i|^{\frac{1}{2}} + \frac{2}{v}\mathbf{1}_i^T(\mathbf{x}^*-\mathbf{y})\mathbf{r}_i) + \mathbf{r}^T\mathbf{r}, \end{aligned} \tag{16}$$

Based on **Proposition 2** of [1], for any $i\in\Omega$, we derive

$$\begin{aligned} & |\mathbf{x}_i^*+\mathbf{r}_i|^{\frac{1}{2}} - |\mathbf{x}_i^*|^{\frac{1}{2}} + \frac{2}{v}\mathbf{1}_i^T(\mathbf{x}^*-\mathbf{y})\mathbf{r}_i \\ &\quad = |\mathbf{x}_i^*+\mathbf{r}_i|^{\frac{1}{2}} - |\mathbf{x}_i^*|^{\frac{1}{2}} - \frac{sign(\mathbf{x}_i^*)}{2|\mathbf{x}_i^*|^{\frac{1}{2}}}\mathbf{r}_i, \end{aligned} \tag{17}$$

and for any $i\in\Omega^c$, we get

$$|\mathbf{r}_i|^{\frac{1}{2}} + \frac{2}{v}\mathbf{1}_i^T(\mathbf{x}^*-\mathbf{y})\mathbf{r}_i \geq |\mathbf{r}_i|^{\frac{1}{2}} - \frac{\sqrt[3]{54}}{2(v\mu)^{\frac{1}{3}}}|\mathbf{r}_i|, \tag{18}$$

Then using the Taylor expansion, for any $i\in\Omega$, we deduce

$$|\mathbf{x}_i^*+\mathbf{r}_i|^{\frac{1}{2}} - |\mathbf{x}_i^*|^{\frac{1}{2}} - \frac{sign(\mathbf{x}_i^*)}{2|\mathbf{x}_i^*|^{\frac{1}{2}}}\mathbf{r}_i = \frac{-{\mathbf{r}_i}^2}{8|\mathbf{x}_i^*+\rho\mathbf{r}_i|^{\frac{3}{2}}}, \tag{19}$$

for the constant $\rho\in(0,1)$. Since $\max_{i\in\Omega}|\mathbf{r}_i| \leq \|\mathbf{r}\|_2 < \beta_0 e$, for any $i\in\Omega$, we have

$$|\mathbf{x}_i^* + \rho \mathbf{r}_i| \geq |\mathbf{x}_i^*| - \rho |\mathbf{r}_i| \geq (1-\beta_0)e, \tag{20}$$

which implies

$$|\mathbf{x}_i^* + \mathbf{r}_i|^{\frac{1}{2}} - |\mathbf{x}_i^*|^{\frac{1}{2}} + \frac{2}{v}\mathbf{1}_i^T(\mathbf{x}^* - \mathbf{y})\mathbf{r}_i \geq \frac{-\mathbf{r}_i^2}{8(1-\beta_0)^{\frac{3}{2}}e^{\frac{3}{2}}}, \tag{21}$$

By Eqs. (16)-(21), it is derived that

$$\begin{aligned}
&\theta_v(\mathbf{x}^* + \mathbf{r}) - \theta_v(\mathbf{x}^*) \\
&\geq \|\mathbf{r}\|^2 + v\sum_{i\in\Omega^c}(|\mathbf{r}_i|^{\frac{1}{2}} - \frac{\sqrt[3]{54}}{2(v\mu)^{\frac{1}{3}}}|\mathbf{r}_i|) - v\sum_{i\in\Omega}\frac{\mathbf{r}_i^2}{8(1-\beta_0)^{\frac{3}{2}}e^{\frac{3}{2}}} \\
&\geq (\|\mathbf{1}_\Omega \mathbf{r}_\Omega\|_2^2 - \frac{v}{8(1-\beta_0)^{\frac{3}{2}}e^{\frac{3}{2}}}\|\mathbf{r}_\Omega\|_2^2) + \|\mathbf{1}_{\Omega^c}\mathbf{r}_{\Omega^c}\|_2^2 \\
&\quad +2(\mathbf{1}_\Omega \mathbf{r}_\Omega)^T\mathbf{1}_{\Omega^c}\mathbf{r}_{\Omega^c} + v\sum_{i\in\Omega^c}(|\mathbf{r}_i|^{\frac{1}{2}} - \frac{\sqrt[3]{54}}{2(v\mu)^{\frac{1}{3}}}|\mathbf{r}_i|) \\
&\geq v\sum_{i\in\Omega^c}(|\mathbf{r}_i|^{\frac{1}{2}} - \frac{\sqrt[3]{54}}{2(v\mu)^{\frac{1}{3}}}|\mathbf{r}_i| - \frac{2}{v}|\mathbf{1}_i{}^T(\mathbf{1}_\Omega \mathbf{r}_\Omega)||\mathbf{r}_i|) \\
&\quad +(\sigma_{\min}(\mathbf{1}_\Omega^T\mathbf{1}_\Omega) - \frac{v}{8(1-\beta_0)^{\frac{3}{2}}e^{\frac{3}{2}}})\|\mathbf{r}_\Omega\|_2^2,
\end{aligned} \tag{22}$$

Since $\|\mathbf{r}\|_2 < \beta_0 e \leq c_{\beta_0} e$, for any $i \in \Omega^c$, we have

$$\begin{aligned}
|\mathbf{r}_i|^{\frac{1}{2}} &\leq \frac{1}{\frac{\sqrt[3]{54}}{2(v\mu)^{\frac{1}{3}}} + \frac{2}{v}\|\mathbf{1}_{\Omega^c}^T\mathbf{1}_\Omega\|_2\beta_0 e} \\
&\leq \frac{1}{\frac{\sqrt[3]{54}}{2(v\mu)^{\frac{1}{3}}} + \frac{2}{v}\|\mathbf{1}_{\Omega^c}^T\mathbf{1}_\Omega\|_2\|\mathbf{r}_\Omega\|_2} \\
&\leq \frac{1}{\frac{\sqrt[3]{54}}{2(v\mu)^{\frac{1}{3}}} + \frac{2}{v}\|\mathbf{1}_{\Omega^c}^T\mathbf{1}_\Omega\mathbf{r}_\Omega\|_2} \\
&\leq \frac{1}{\frac{\sqrt[3]{54}}{2(v\mu)^{\frac{1}{3}}} + \frac{2}{v}\max_{i\in\Omega^c}|\mathbf{1}_i^T\mathbf{1}_\Omega\mathbf{r}_\Omega|} \\
&\leq \frac{1}{\frac{\sqrt[3]{54}}{2(v\mu)^{\frac{1}{3}}} + \frac{2}{v}|\mathbf{1}_i^T\mathbf{1}_\Omega\mathbf{r}_\Omega|},
\end{aligned} \tag{23}$$

Therefore,

$$\begin{aligned}
&|\mathbf{r}_i|^{\frac{1}{2}} - \frac{\sqrt[3]{54}}{2(v\mu)^{\frac{1}{3}}}|\mathbf{r}_i| - \frac{2}{v}|\mathbf{1}_i{}^T(\mathbf{1}_\Omega\mathbf{r}_\Omega)||\mathbf{r}_i| \\
&= (1 - (\frac{\sqrt[3]{54}}{2(v\mu)^{\frac{1}{3}}} + \frac{2}{v}|\mathbf{1}_i{}^T(\mathbf{1}_\Omega\mathbf{r}_\Omega)|)|\mathbf{r}_i|^{\frac{1}{2}})|\mathbf{r}_i|^{\frac{1}{2}} \geq 0,
\end{aligned} \tag{24}$$

By Eqs. (22)-(24), we derive

$$\theta_v(\mathbf{x}^* + \mathbf{r}) - \theta_v(\mathbf{x}^*) \geq (\sigma_{\min}(\mathbf{1}_\Omega^T\mathbf{1}_\Omega) - \frac{v}{8(1-\beta_0)^{\frac{3}{2}}e^{\frac{3}{2}}})\|\mathbf{r}_\Omega\|_2^2, \tag{25}$$

Due to $\beta_0 < \beta^*$, this suggests

$$\sigma_{\min}(\mathbf{1}_\Omega^T\mathbf{1}_\Omega) - \frac{v}{8(1-\beta_0)^{\frac{3}{2}}e^{\frac{3}{2}}} \geq \sigma_{\min}(\mathbf{1}_\Omega^T\mathbf{1}_\Omega) - \frac{v}{8(1-\beta^*)^{\frac{3}{2}}e^{\frac{3}{2}}} = 0, \tag{26}$$

Besides,

$$\theta_v(\mathbf{x}^* + \mathbf{r}) - \theta_v(\mathbf{x}^*) \geq 0, \tag{27}$$

Consequently, $\mathbf{x}^*$ is a local minimizer of Eq. (1). The proof of **Theorem 1** is completed.

To sum up, **Lemma 2** and **Theorem 1** provide a theoretical guarantee for the convergence proof of Eq. (2).

III. More Experimental Results

A. Color Correction Validation

A simple yet effective color correction based on statistical method [4] is adopted to address color distortions of degraded underwater images. Fig. 1 shows the enhanced results by the color correction method [4] and the proposed method, and the corresponding three-dimensional (3D) histograms are plotted to strengthen the illustration. Based on the color correction scheme, our method yields better results in terms of contrast and details enhancement in various types of underwater scenes. Meanwhile, the 3D histograms of the color correction method [4] and the proposed method are more evenly distributed in the whole range, while the histogram distributions of raw images are more concentrated around particular values or ranges. The intensities of the color-corrected images are redistributed in a range where image under-enhancement and over-enhancement can be averted. These results suggest that the color correction method [4] is a favorable preprocessing module that recovers authentic colors and naturalness for our model.

B. Convergence Analysis

The convergence of the proposed optimization algorithm is experimented on underwater images with different sizes 254×254, 412×550, 950×1800, 2112×2816. The relationship curves of relative errors ($\boldsymbol{\varepsilon}_{\mathbf{R}} = \|\mathbf{R}^k - \mathbf{R}^{k-1}\|/\|\mathbf{R}^{k-1}\|$), ($\boldsymbol{\varepsilon}_{\mathbf{I}} = \|\mathbf{I}^k - \mathbf{I}^{k-1}\|/\|\mathbf{I}^{k-1}\|$) versus the iteration number k are plotted in Fig. 2(a) and (b) where an intuitive illustration of convergence speed of our method is presented. As can be seen, the convergence rate is fast and independent of image size, and the errors $\boldsymbol{\varepsilon}_{\mathbf{R}}$ and $\boldsymbol{\varepsilon}_{\mathbf{I}}$ are less than 0.01 after 5 iterations. For most images, our algorithm stably converges when reaching 5 iterations as the maximum iteration T sufficient to yield decent results in our experiments. The convergence phenomenon is due to our optimization algorithm that splits the complex energy minimization problem into a couple of simple subproblems that separately optimize reflectance $\mathbf{R}$ and illumination $\mathbf{I}$.

C. Parameter Evaluation

We study the effect of regularization parameters λ_1, λ_2, ζ_1 and ζ_2 on our model. The empirical parameters are set to be $\lambda_1 = 1e-4$, $\lambda_2 = 1e-3$, $\zeta_1 = 1e-5$, $\zeta_2 = 1e-3$ as shown in Fig. 3(c) and (h). First, Fig. 3(a-c) shows enhanced images, enhanced reflectance and enhanced illumination when the variations of λ_1 between $1e-5$ and $1e-3$, and it is noted that UIQM [9] and UCIQE [10] are best when λ_1 reaches $1e-4$, meanwhile, the visual difference of enhanced images is invisible, and insignificant discrepancy is shown in enhanced reflectances and illuminations respectively. Fig. 3(c-e) shows the counterparts when the variations of λ_2 between

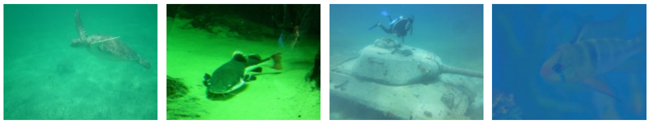

(a) Raw images.

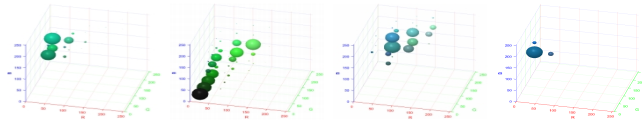

(b) 3D histograms of (a).

(c) Color correction [4].

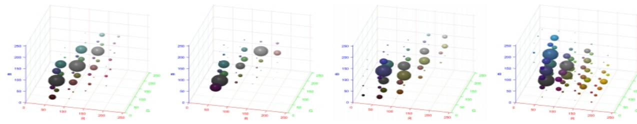

(d) 3D histograms of (c).

(e) Our enhancement.

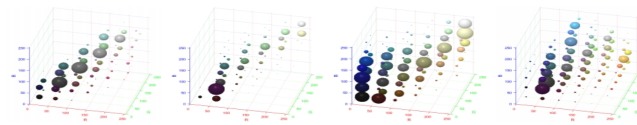

(f) 3D histograms of (e).

Fig. 1: Color correction [4], our enhancement, and corresponding three-dimensional (3D) histogram. Based on the color correction [4], our retinex variational enhancement method (e) yields better results in terms of contrast and details enhancement against various underwater scenes. The 3D histograms of the color correction method [4] (d) and the proposed model (f) are more evenly distributed in the whole range, while the histogram distributions of raw images (b) are more concentrated around particular values or ranges. When compared (f) with (d), our method has more uniform 3D distributions as well as more types of color balls, which suggests the superiority of our method in terms of contrast promotion and color recovery.

$1e-4$ and $1e-2$. UIQM and UCIQE are maximum when λ_2 is $1e-3$, and the invisible difference is in comparison of enhanced results. Then, the effect of parameters ζ_1 and ζ_2 is probed, and comparison results are respectively shown in Fig. 3(f-h) and (h-j). The variation tendency of ζ_1 and ζ_2 is similar to those of λ_1 and λ_2, and the default settings $\zeta_1 = 1e-5$ and $\zeta_2 = 1e-3$ are better for UIQM and UCIQE. Besides, the enhanced illumination becomes bright when $\zeta_2 = 1e-4$ and dark when $\zeta_2 = 1e-2$, because ζ_2 controls spatial linear smoothness of the illumination. It is worth noting that the enhanced results are almost unchanged when these parameters vary, and the maximum changes of UIQM$|$UCIQE are $0.009|0.009$ for the variations of λ_1, λ_2, ζ_1 and $0.057|0.013$ for that of ζ_1, which suggests very small changes of UIQM and UCIQE. In most cases, the empirical setting of regularization parameters generates decent results.

D. Application Tests

We complement more results of different methods on underwater image segmentation and underwater keypoint detection. As shown in Fig. 4, more consistent and accurate segmentation results are produced by our method, which outperforms those of other methods, and our superiority is obvious in foreground objects and segmentation boundaries. As displayed in Fig. 5, our method achieves more keypoint numbers than other methods, and recovers more crucial underwater image features that are helpful to subsequent vision tasks. These tests demonstrate the effectiveness of our method.

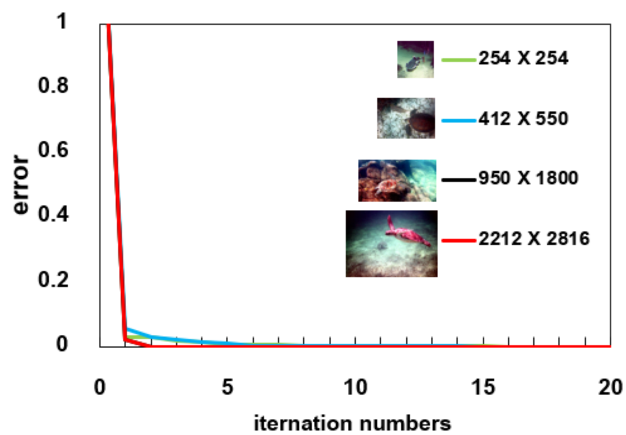

(a) $\varepsilon_{\mathbf{R}}$

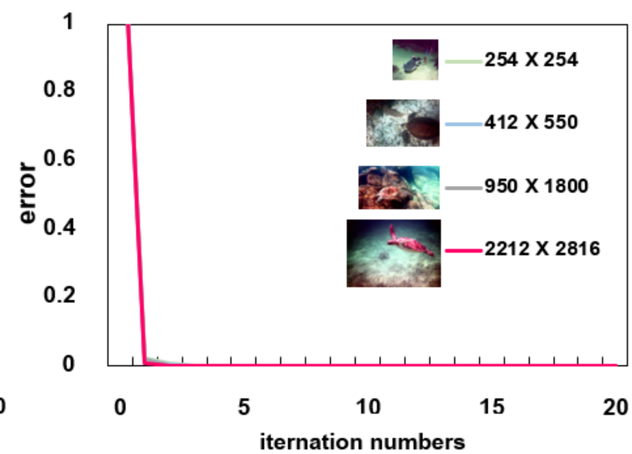

(b) $\varepsilon_{\mathbf{I}}$

Fig. 2: The relation between the errors ($\varepsilon_{\mathbf{R}}$, $\varepsilon_{\mathbf{I}}$) and the iteration numbers (k).

(a) 4.783|0.635 (b) 4.784|0.635 (c) 4.792|0.644 (d) 4.783|0.635 (e) 4.783|0.635

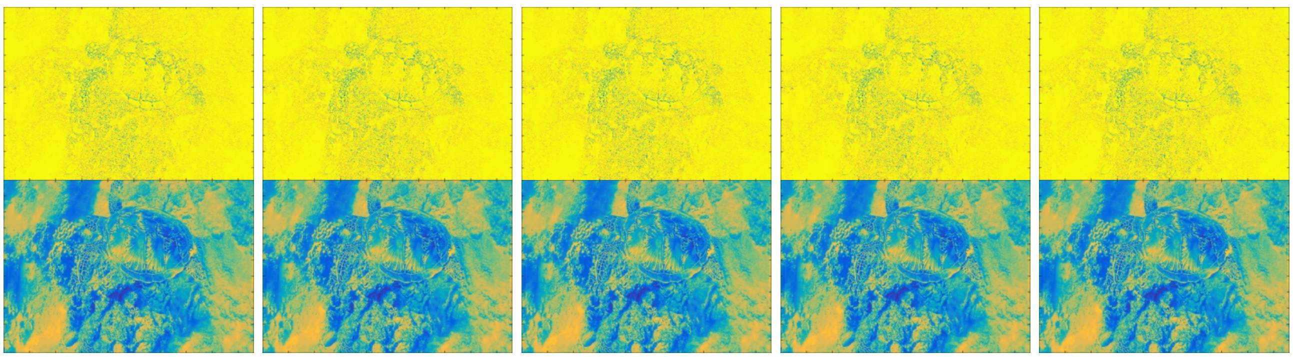

(f) 4.783|0.635 (g) 4.783|0.635 (h) 4.792|0.644 (i) 4.764|0.635 (j) 4.735|0.631

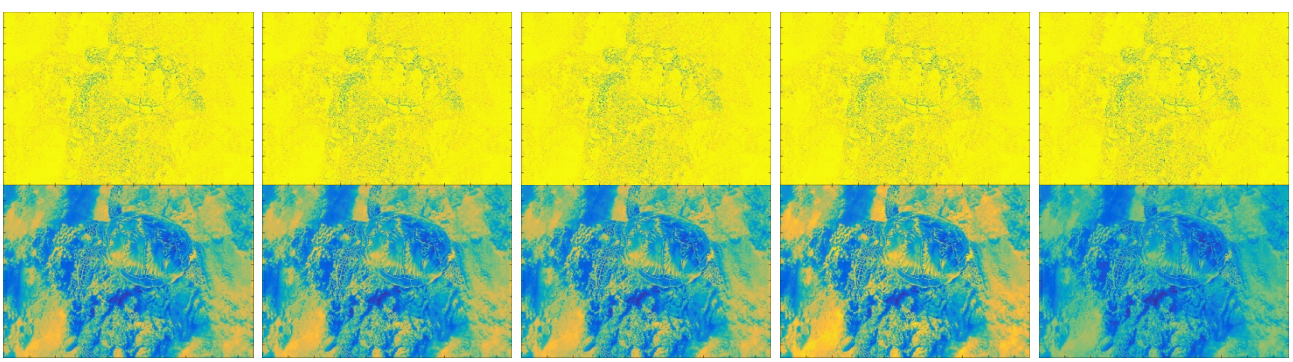

Fig. 3: Parameter evaluation. Row 1-3: the effect of regularization parameters λ_1 and λ_2. (a) $\lambda_1 = 1e-5$, $\lambda_2 = 1e-3$. (b) $\lambda_1 = 1e-3$, $\lambda_2 = 1e-3$. (c) default $\lambda_1 = 1e-4$, $\lambda_2 = 1e-3$. (d) $\lambda_1 = 1e-4$, $\lambda_2 = 1e-4$, (e) $\lambda_1 = 1e-4$, $\lambda_2 = 1e-2$. Row 4-6: the effect of regularization parameters ζ_1 and ζ_2. (f) $\zeta_1 = 1e-6$, $\zeta_2 = 1e-3$. (g) $\zeta_1 = 1e-4$, $\zeta_2 = 1e-3$. (h) default $\zeta_1 = 1e-5$, $\zeta_2 = 1e-3$. (i) $\zeta_1 = 1e-5$, $\zeta_2 = 1e-4$. (j) $\zeta_1 = 1e-5$, $\zeta_2 = 1e-2$. For each group, from top to bottom: enhanced image, enhanced reflectance, enhanced illumination. UIQM|UCIQE are correspondingly shown below.

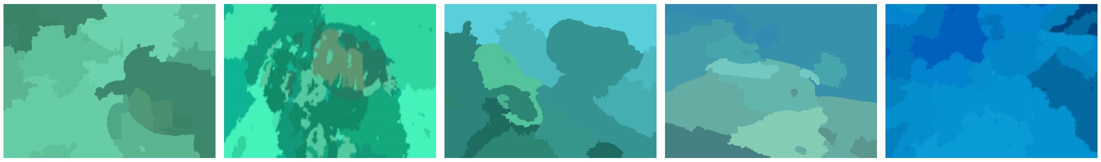

(a) Raw

(b) IBLA [5]

(c) CBF [6]

(d) GDCP [7]

(e) Waternet [8]

(f) Ours

Fig. 4: Underwater image segmentation.

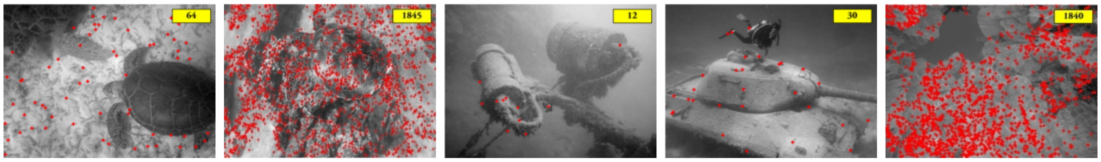

(a) Raw

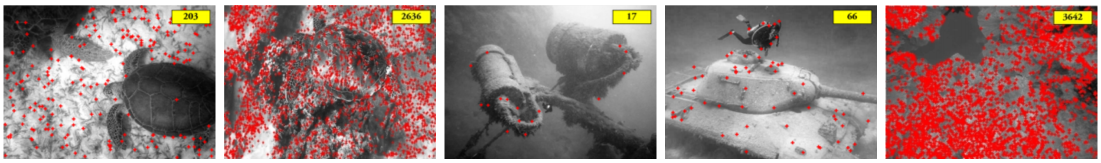

(b) IBLA [5]

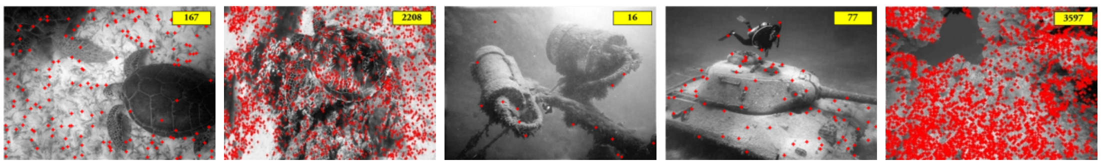

(c) CBF [6]

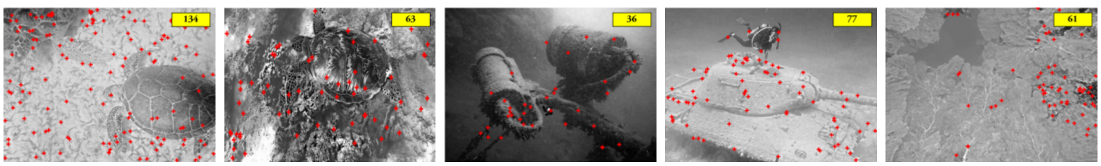

(d) GDCP [7]

(e) Waternet [8]

(f) Ours

Fig. 5: Underwater keypoint detection. The best result is in red under each case.

REFERENCES

[1] J. Zeng, S. Lin, Y. Wang, and Z. Xu, "$L_{1/2}$ regularization: Convergence of iterative half thresholding algorithm," *IEEE Trans. Signal Process.*, vol. 62, no. 9, pp. 2317-2329, 2014.

[2] Z. Xu, X. Chang, F. Xu, and H. Zhang, "$L_{1/2}$ regularization: A thresholding representation theory and a fast solver," *IEEE Trans. Neural Netw. Learn. Syst.*, vol. 23, no. 7, pp. 1013-1027, 2012.

[3] R. H. Chan, H. Liang, S. Wei, M. Nikolova, and X. C. Tai, "High-order total variation regularization approach for axially symmetric object tomography from a single radiograph," *Inverse Probl. Imag.*, vol. 9, no. 1, pp. 55-77, 2015.

[4] X. Fu, P. Zhuang, Y. Huang, Y. Liao, X. P. Zhang, and X. Ding, "A retinex-based enhancing approach for single underwater image," *IEEE Intl. Conf. Image Process.*, 2014, pp. 4572-4576.

[5] Y. T. Peng and P. C. Cosman, "Underwater image restoration based on image blurriness and light absorption," *IEEE Trans. Image Process.*, vol. 26, no. 4. pp. 1579-1594, 2017.

[6] C. O. Ancuti , C. Ancuti, C. D. Vleeschouwer, and P. Bekaert, "Color balance and fusion for underwater image enhancement," *IEEE Trans. Image Process.*, vol. 27, no. 1, pp. 379-393, 2018.

[7] Y. T. Peng, K. Cao, and P. C. Cosman, "Generalization of the dark channel prior for single image restoration," *IEEE Trans. Image Process.*, vol. 27, no. 6. pp. 2856-2868, 2018.

[8] C. Li, C. Guo, W. Ren, R. Cong, J. Hou, S. Kwong, and D. Tao, "An underwater image enhancement benchmark dataset and beyond," *IEEE Trans. Image Process.*, vol. 29. pp. 4376-4389, 2019.

[9] K. Panetta, C. Gao, and S. Agaian, "Human-visual-system-inspired underwater image quality measures," *IEEE J. Ocean Eng.*, vol. 41, no. 3, pp. 1-11, 2015.

[10] M. Yang and A. Sowmya, "An underwater color image quality evaluation metric," *IEEE Trans. Image Process.*, vol. 24, no. 12, pp. 6062-6071, 2015.